LRT, a tendon-specific leucine-rich repeat protein, promotes muscle-tendon targeting through its interaction with Robo

Bess Wayburn and Talila Volk*

Correct muscle migration towards tendon cells, and the adhesion of these two cell types, form the basis for contractile tissue assembly in the *Drosophila* embryo. While molecules promoting the attraction of muscles towards tendon cells have been described, signals involved in the arrest of muscle migration following the arrival of myotubes at their corresponding tendon cells have yet to be elucidated. Here, we describe a novel tendon-specific transmembrane protein, which we named LRT due to the presence of a leucine-rich repeat domain (LRR) in its extracellular region. Our analysis suggests that LRT acts non-autonomously to better target the muscle and/or arrest its migration upon arrival at its corresponding tendon cell. Muscles in embryos lacking LRT exhibited continuous formation of membrane extensions despite arrival at their corresponding tendon cells, and a partial failure of muscles to target their correct tendon cells. In addition, overexpression of LRT in tendon cells often stalled muscles located close to the tendon cells. LRT formed a protein complex with Robo, and we detected a functional genetic interaction between Robo and LRT at the level of muscle migration behavior. Taken together, our data suggest a novel mechanism by which muscles are targeted towards tendon cells as a result of LRT-Robo interactions. This mechanism may apply to the Robo-dependent migration of a wide variety of cell types.

KEY WORDS: *Drosophila*, Leucine-rich repeat, Robo, Muscle, Tendon

INTRODUCTION

The correct migration and adhesion between cells of different origin is essential for tissue morphogenesis. The development of the *Drosophila* embryonic contractile tissue established by the migration and adhesion of muscles towards their corresponding tendon cells has served as a model through which to study various aspects of tissue assembly, including guided muscle migration and the formation of the myotendinous junction (Schnorrer and Dickson, 2004; Volk, 1999). Somatic myotubes produced at distinct embryonic sites migrate towards specific ectodermal cells, termed tendon cells, defined in *Drosophila* by the expression of the transcription factor Stripe (Volk and VijayRaghavan, 1994; Williams and Caveney, 1980). Stripe is an EGR-like transcription factor that defines tendon cell identity in the ectoderm (Frommer et al., 1996). Stripe is both necessary and sufficient to promote muscle migration towards tendon cells (Becker et al., 1997; Volk and VijayRaghavan, 1994; Vorbruggen and Jackle, 1997). In addition, Stripe is required for the maturation of tendon cells following their attachment to muscles (Volohonsky et al., 2007). Subsequently, myotubes form integrin-mediated hemi-adherens-type junctions with tendon cells at both their ends so that each myotube is stretched between two ectodermal tendon cells (Bokel and Brown, 2002). This organization enables the typical wave-like movement of the hatched crawling larvae.

Muscle migration towards tendon cells is a multistep process in which founder cells first move apart from each other; then, during and following muscle fusion, each myotube directs its leading edge towards a specific tendon cell in response to guidance cues provided by the tendon (Schnorrer and Dickson, 2004; Volk, 1999). Often, the migrating myotube first establishes contact with a tendon cell located at the posterior segmental border, and then extends its opposite end towards a tendon cell located at the anterior segment border. Following the arrival of the muscle's leading edge to this tendon cell, its migration is arrested and the myotendinous junction is formed.

Tendon cells are crucial in providing guidance for muscle migration. In the absence of such signals (e.g. in *stripe* mutants), muscles lose their directional migration and fail to attach to tendon cells, leading to a complete disruption of the muscle pattern and failure of the larvae to move (Frommer et al., 1996). Positive guidance cues produced by tendon cells that act to attract muscles towards tendon cells were described. These include proteins directing axon migration, such as Slit and Syndecan (Kramer et al., 2001; Steigemann et al., 2004). Signals mediating the arrest of muscle migration once it has reached its targeted tendon cell have not yet been described.

Slit is secreted by tendon cells under the regulation of Stripe (Kramer et al., 2001; Volohonsky et al., 2007), whereas Roundabout (Robo) and Robo2 (Leak – FlyBase) are expressed in specific muscles (Kramer et al., 2001). Slit expression is not unique to the muscle/tendon junction, and this protein also mediates axonal pathfinding in the central nervous system (Dickson and Gilestro, 2006). However, unlike the Slit-Robo interactions in the nervous system, where Robo appears to mediate the repulsion or turning away of the axonal leading edge, muscles respond to Slit in two distinct fashions (Kramer et al., 2001). The ventral oblique muscles, which migrate ventrally, are first repulsed from the ventral midline in response to Slit, and in later developmental stages they are attracted to Slit provided by the segmental border tendon cells. Consequently, in *slit* or *robo* mutant embryos, the ventral oblique muscles cross the ventral midline, resulting in an aberrant pattern. Midline rescue of Slit in *slit* mutant embryos exhibits a muscle phenotype in which the ventral longitudinal muscles fail to attach to the tendon cells at the segmental border tendon cells. In addition, ectopic expression of Slit in the two rows of cells in the Engrailed domain leads to attraction of the ventral longitudinal muscles to this ectopic site (Kramer et al., 2001).

Department of Molecular Genetics, Weizmann Institute of Science, Rehovot 76100, Israel.

*Author for correspondence (lgvolk@weizmann.ac.il)

DEVELOPMENT

In an effort to identify additional tendon-specific signals essential for the guidance of migrating muscles towards tendon cells, we recently performed a microarray screen for Stripe downstream targets. One of the genes recovered was CG11136, a novel gene that encodes a type1 transmembrane protein containing a leucine-rich repeat (LRR) domain in its extracellular region.

LRR domains are formed by a string of consecutive leucine-rich repeats separated by variable inter-strand segments. This domain has been implicated in protein-protein interactions (Bella et al., 2008). Several transmembrane or secreted LRR proteins have been described in *Drosophila*, including Tartan, Capricious and others (Dolan et al., 2007; Kurusu et al., 2008). Mutants in these genes exhibit a wide range of phenotypes, depending on their tissue-specific distribution. However, they share a common function in cell-cell recognition events (Blair, 2001; Kohsaka and Nose, 2009; Krause et al., 2006; Milan et al., 2002; Milan et al., 2005; Milan et al., 2001; Sakurai et al., 2007). Two additional LRR proteins, Haf and CG8561 (Convoluted – FlyBase), expressed by muscle cells, affect motor axon recognition of specific muscles (Kurusu et al., 2008). The molecular basis for the activity of these proteins is yet to be elucidated.

Here, we show that CG11136 is a tendon-specific LRR transmembrane protein that is required for the establishment of the correct embryonic muscle pattern. In its absence, specific muscles do not extend properly to their attachment sites, and other muscles do not arrest their migration behavior. Due to its tendon-specific distribution we named the CG11136 protein 'Leucine-rich tendon-specific protein' (LRT). We show that LRT forms a protein complex with Robo, and that these proteins functionally interact, thereby affecting the extent of muscle extension towards tendon cells. Taken together, our data suggest a model in which the association of LRT with Robo receptors at the level of the muscle-tendon junction is essential for better targeting of muscles to their tendon cells as well as arrest of muscle migratory behavior.

MATERIALS AND METHODS
Fly stocks
The following fly stocks were used: *yw*, *stripe-gal4* (G. Morata, Madrid, Spain), *mef2gal4*, *actin-gal4*, UAS-*slit*, *Df*(2R)BSC403 and *Df*(2R)Exel7164 (Bloomington Stock Center); *UAS-lrt-gfp* and *UAS-lrt-ntd-gfp* were created in the lab (injected in flies by Genetic Services); UAS-CD8-GFP and *5053-gal4*/TM3 (a gift from Frank Schnorrer, Max Planck Institute of Biochemistry, Martinsried, Germany); *44991*-expressing RNAi against LRT (Vienna Drosophila Research Center); *robo^1/cyo sli^2/cyo* (B. Dickson, IMP, Vienna, Austria); *UAS-Robo-RNAi;Robo2-RNAi;Robo3-RNAi* (a gift from V. Rodrigeus, NCBS, Bangalore, India).

The fly lines *Df*(2R)BSC403/cyo;uas-lrt-gfp and *Df*(2R)BSC403/cyo;srgal4/TM6 were created to enable rescue of *Df*(2R)BSC403. In all cases, a Kr-GFP marked CyO balancer was used to identify the homozygous mutants.

For the analysis of the phenotype of Muscle 12 we used flies with the following genotype:Df(2R)BSC403/CyO,KrGFP; 5053-gal4,UAS-CD8GFP/TM6. The GFP pattern of the 5053-gal4 is distinct from that of the Kr-GFP, enabling the identification of the homozygous mutants.

For the rescue of the flies above we crossed Df(2R)BSC403, UAS-LRT-GFP/CyO,Kr-GFP; 5053-gal4/TM6 X Df(2R)BSC403/CyO,Kr-GFP; sr-gal4/TM6. The GFP was detected in three distinct sites: in tendon cells, in muscle 12 and in Kruppel (Kr) pattern. The homozygous rescued mutants were identified by negative staining of the Kr pattern, and positive GFP staining of muscle 12 as well as tendon cells.

Constructs
The Gateway Cloning Technology (Invitrogen Life Technologies, USA) was used to produce the following constructs: full *lrt* was amplified for insertion into the Gateway pDonr-201 vector with primers 5′-GGGGACAAGTTTGTACAAAAAAGCAGGCTCTCGCACGCT GATAAAGAGG-3′ (forward) and 5′-GGGGACCACTTTGTACAA-GAAAGCTGGGTTCAGGCTCGTCGTTGCCTG-3′ (reverse). The insert was then transferred to destination vector pTWG, which contains a 5′ UAS promoter sequence and a 3′ GFP tag. This construct was used to drive GFP-labeled LRT expression in cells as well as in transgenic flies.

UAS-lrt-ntd-gfp was created with the same forward primer as the complete LRT, and the following reverse primer: 5′-GGGGACC-ACTTTGTACAAGAAAGCTGGGTTCGAATCAATGACCGTGTAG-3′.

pUAST-Robo-HA construct was obtained from B. Dickson (IMP, Vienna).

5′ RACE of CG11136
The 5′ ends of mRNAs extracted from an embryo collection of 10- to 16-hour-old embryos were specifically capped with a known sequence. Primers specific to the cap as well as to the known region of LRT (at its 5′ region) were then used to amplify the potential unknown 5′ region. A fragment of 520 bp was identified that contained the 5′ UTR region of LRT as well as part of its coding sequence. This fragment was fused to the rest of LRT cDNA and was used in all further experiments (rescue, overexpression and immunoprecipitation).

In situ hybridization
A DNA probe was created with following primers: 5′-CCAATGACCT-CAAGGATCC-3′ (forward) and 5′-GTGTGAGGCAGATCGCAT-3′ (reverse). In situ hybridization was performed as described (Subramanian et al., 2007).

Immunochemical reagents
The following primary and secondary antibodies were used: mouse anti-GFP antibody (Roche Diagnostics); mouse monoclonal anti-HA (11583816001, Roche, Switzerland) at 1:200 for immunostaining and 1:1000 for western blot; anti-Myosin heavy chain (P. Fisher, Stony Brook, NY, USA) at 1:500 for immunostaining. Anti βPS-integrin (Hybridoma Center) was used at 1:2 for immunostaining. Guinea pig anti-Sr (produced in our lab) was used 1:200 for immunostaining. Mouse anti-Robo [Hybridoma Center and S. Kramer (UMDNJ-Robert Wood Johnson Medical School, NJ, USA)] was used at 1:10 for immunostaining. Chick anti-GFP was used at 1:500 for immunostaining. Secondary antibodies conjugated with Cy3, Cy5 and FITC raised against guinea pig, rat, mouse and rabbit were purchased from Jackson ImmunoResearch Laboratories.

Rat anti-LRT (see Results) was raised against a unique sequence in the N-terminal region of the protein and was used at 1:200 for immunostaining

SR+ and S2 Schneider cell transfections
Drosophila S2 cells were maintained in Schneider's Drosophila Medium (01-150-1A, Biological Industries, Israel) + 10% FBS (12657-029, Gibco, USA) at 25°C. Cells were transfected using the Escort IV transfection reagent (L3287, Sigma-Aldrich, USA) according to the manufacturer's instructions. The transfected cells were incubated for 24 hours before use for protein extraction or immunostaining.

Immunofluorescent staining procedures
The embryos were dechorionated and fixed in 4% formaldehyde (FA). Following fixation, the embryos were devitellinated with methanol, washed in PTW and blocked in 10% BSA in PTW for 1 hour. Embryos were incubated with the primary antibody over night. Then the embryos were washed with PTW, secondary antibody was added for 2 hours, and they were washed again and dehydrated in 80% glycerol.

For heat fixation, the embryos were collected from the sieve using a spatula and added to 5 ml of a boiling solution of 0.7% NaCl and 0.04% Triton-X in a 50 ml Eppendorf tube. After 5 seconds, the tube was transferred to ice and 20 ml of ice-cold NaCl/Triton solution was added. The embryos were incubated on ice for 15 minutes and then transferred to a 2 ml Eppendorf tube. The Triton/salt solution was removed, and the vitelline membrane removed by vigorous shaking in a 1:1 heptane:methanol solution. The embryos were then incubated in methanol for at least 1 hour before normal rehydration and staining as described above.

Immunoprecipitation and western analysis

Transfected S2 cells were harvested by centrifugation in a 15 ml tube at 1200RPM to remove the media. The pelleted cells were then washed with PBS. The cells were lysed in NP40 buffer (10 mM Tris-Cl pH 8.0, 150 mM NaCl, 0.1% NP40) + protease inhibitors (Sigma P 8340) and incubated on ice for 10 minutes. After pelleting the debris, the crude extract was added to Protein G PLUS-Agarose beads (sc-2003, Santa-Cruz Biotechnology, USA) preloaded with the anti-GFP antibody overnight at 4°C. The mixture was allowed to incubate overnight at 4°C in a rotating arm. The beads were pelleted, washed in NP40 buffer and boiled in sample buffer for use in the western analysis. Western analysis was performed according to standard procedures described (Volk, 1992).

Stripe microarray

Embryos aged 10-15 hours after egg laying were collected, either of wild type or carrying *69B-gal4::UAS-stripeB* constructs. The total RNA was extracted using the Macherey-Nagel NucleoSpin RNA II mini kit, following the protocol, and then kept at –70°C. Total RNA was prepared independently five times from embryos of each genetic background in order to better normalize the age of these embryo populations. The RNA samples were then collected and concentrated to give 1 mg of total RNA using the RNA cleanup RNeasy Mini Kit (Qiagen). The probe preparation, cDNA synthesis, cRNA reactions and hybridization with Affymetrix high-density oligonucleotide arrays for *Drosophila melanogaster* was carried out in the Weizmann Institute microarray unit. The microarray experiment was repeated four times. CG11136 (LRT) was consistently elevated in the order of $2^{0.8}$.

Confocal microscopy

Visualization was performed with a Zeiss LSM 510Meta or a Zeiss LSM710 confocal system. The fluorescent digital images were processed using Adobe PhotoShop CS.

RESULTS
LRT is a tendon-specific protein that is positively regulated by Stripe

In a microarray screen designed to identify genes that are expressed downstream of Stripe (for details see Materials and methods), we identified *CG11136*. The CG11136 open reading frame sequence contains a signal peptide, a leucine-rich repeat domain, a transmembrane domain and a small cytoplasmic domain at its C-terminal end, suggesting that it is a type I transmembrane domain protein (Fig. 1A). In situ hybridization with an antisense RNA probe for *CG11136* indicated an expression pattern similar to that of Stripe, suggesting a tendon-specific distribution (Fig. 1B,C). Thus, we named the CG11136 gene product Leucine-rich tendon-specific protein (LRT). The mRNA expression of LRT was detected from embryonic stage 12 and persisted to late stage 16. Overexpression of Stripe in the Engrailed domain (driven by *en-gal4*) led to expression of *lrt* in the engrailed domain, which is wider by an additional row of cells relative to the Stripe-positive cell row in the segmental border (Fig. 1D,D′), indicating that *lrt* expression can be promoted by Stripe. However, we found that the protein coded by *lrt* was still expressed in *stripe* mutant embryos (data not shown), suggesting an earlier transcriptional regulation of this gene, similar to some of the *stripe* downstream genes described previously (Chanana et al., 2007; Subramanian et al., 2007).

An antibody was raised against the unique extracellular domain of LRT, using as an antigen a recombinant fragment that excluded the LRR domain, to prevent cross-reactivity with other LRR proteins. Staining of embryos with this antibody revealed a prominent expression pattern of LRT specifically in tendon cells (Fig. 1E,F,G). The intensity of staining varied between the different types of tendons, but it appeared that all tendons were positive for LRT staining. LRT protein staining was detected only at relatively late embryonic stages (stages 15-16 and beyond) following the
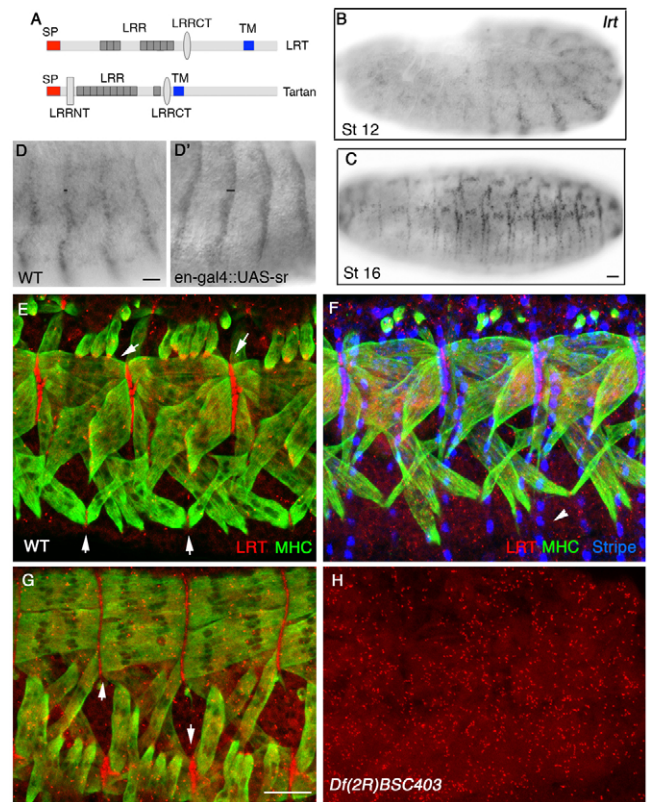

Fig. 1. LRT is expressed in tendon cells. (**A**) The domain structure of LRT compared with that of Tartan, a *Drosophila* transmembrane LRR protein. (**B-D′**) The distribution of *lrt* mRNA in whole embryos is demonstrated by in situ hybridization with an *lrt*-specific probe of wild-type embryos at stage 12 (B) and stage 16 (C), as well as in embryos at stage 12-13, either wild type (D) or overexpressing Stripe driven by the *en-gal4* driver (D′). Note that the labeling of *lrt* in D′ is slightly wider than in D (compare bars), representing an additional row of cells of the Engrailed domain. (**E-G**) The distribution of LRT protein is demonstrated in wild-type embryos at stage 16 labeled for LRT (red, E,F,G), Myosin heavy chain (MHC; green, E,F,G), and Stripe (blue, F). Ventral (E,F) and dorsal (G) views of the embryo are shown. LRT is detected in all the tendon cells expressing Stripe that are bound to muscles (arrows in E,G), but not in cells that are not bound to muscles (F, arrowhead). (**H**) Embryo homozygous for Df(2R)BSC403, which uncovers the *lrt* gene, labeled for LRT (red) and showing no staining. Scale bars: 20 μm in C,D,G.

establishment of muscle-tendon attachment (Fig. 1E; Fig. 2). Tendon cells of embryos at stages 13-14, which do not yet bind to muscles, did not exhibit positive staining for LRT protein (not shown), although these cells expressed *lrt* mRNA (see Fig. 1B). It is possible that the antibody was not sensitive enough to detect low protein levels of LRT in these cells. The pattern of LRT staining appeared either as an oval patch on the tendon membrane (e.g. on the ventral longitudinal muscles; see Fig. 1E, Fig. 2A), or as a line (e.g. Fig. 2G). Significantly, LRT accumulated only at the sites of muscle tendon attachment (Fig. 2C, arrowhead), and not on tendon cells that do not bind muscles (Fig. 2C, arrow). To verify the localization of LRT along the tendon cell membrane, we double-labeled embryos with anti-LRT and a tendon-specific membrane marker (CD8-GFP). Single confocal optical sections of the tendons of these embryos showed that LRT was completely absent from the apical surfaces of the tendon cell (not shown) and was detected only at the basal
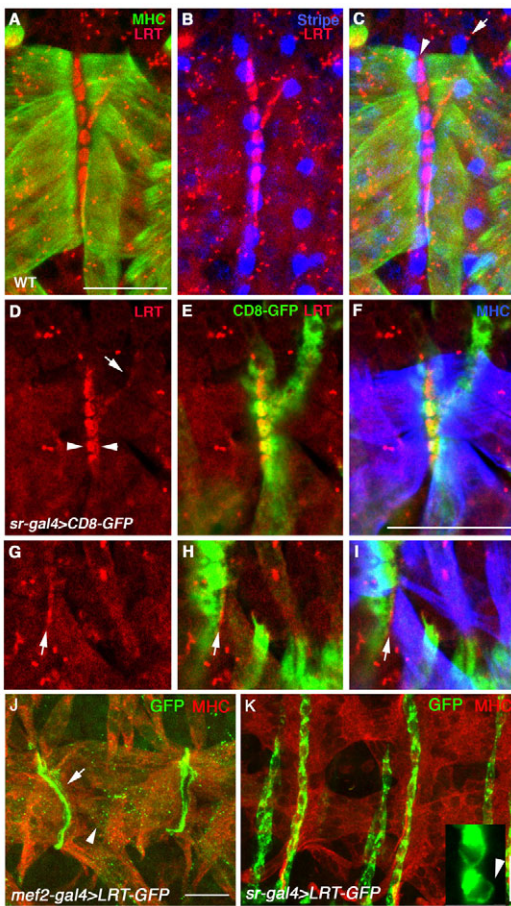
Fig. 2. LRT accumulates at the surfaces of the tendon cell corresponding to muscle ends. (**A-C**) Whole-embryo staining of a wild-type embryo labeled for Myosin heavy chain (MHC; green, A,C), LRT (red, A-C) and Stripe (blue, B,C), showing the association of LRT with the muscle ends. (**D-I**) Single confocal optical sections of an embryo expressing tendon-specific membrane CD8-GFP and stained for GFP (green, E,F,H,I), LRT (red D-I) and MHC (blue, F,I), showing a partial overlap between GFP and LRT. LRT distribution is patchy (arrowheads in D), or appears as a line corresponding to muscle ends (arrows in D,G,H,I). (**J**) Embryo ectopically expressing LRT-GFP (green) in muscles (red) showing its accumulation at the muscle ends (arrow) or in intracellular vesicles (arrowhead). (**K**) Embryo expressing LRT-GFP (green) in tendon cells. Muscles are stained with an anti-MHC antibody (red). (Inset) Arrowhead indicates membrane association of LRT in two highly magnified tendon cells. Scale bars: 20 μm in A,F,J,K.

surfaces of the tendon cells in regions where muscle ends are observed (Fig. 2D-I). In addition to the tendon-specific staining of LRT, we detected small dots along the entire body of the embryo. These dots represent non-specific staining as they also appeared in embryos homozygous for *Df(2R)BSC403*, which uncovers LRT, whereas the tendon-specific LRT staining was eliminated in this mutant (Fig. 1H).

In addition, we created an LRT-GFP fusion construct (in which the GFP is fused to the cytoplasmic tail of LRT), and expressed it in tendons as well as in muscle cells. In tendons, the LRT-GFP fusion protein exhibited clear surface staining (in addition to a patchy intracellular expression pattern) of the tendon cells (Fig. 2K, inset, arrowhead). When expressed in muscles, LRT-GFP accumulated at the muscle-tendon junction site in addition to small dots presumably

representing vesicle staining (Fig. 2J, arrow and arrowhead correspondingly). This suggests that LRT-GFP is exported and capable of accumulating in the muscle ends. These results indicate that LRT is a tendon-specific protein that is positively regulated by Stripe and is localized at the surface of the tendon cell membrane facing muscle ends.

LRT is required for formation of the correct embryonic somatic muscle pattern

To elucidate the function of LRT, we analyzed the phenotype of embryos homozygous for a deficiency that uncovers *lrt* together with an additional 17 genes: *Df(2R)BSC403* (for details of the other 16 genes see Fig. S1 in the supplementary material). The overall muscle pattern in these embryos appeared normal. However, we detected a specific phenotype in the ventral oblique muscles, whereby in 75% (*n*=15) of the mutant embryos two to four segments showed misguided extension of ventral oblique muscle 4 (VO4/muscle 31) and ventral acute muscle 3 (VA3/muscle 18) (arrowheads in Fig. 3B), whereas only 14% of wild-type embryos showed abnormal VO4/VA3 extension in a single segment (*n*=42) (see also Table 1). In addition, in mutant flies, thin cellular extensions were detected at the edges of most of the ventral muscles (arrows in Fig. 3B). Significantly, both phenotypes were rescued in 100% (*n*=11) of the mutant embryos following tendon-specific expression of full-length LRT-GFP (Fig. 3C), indicating that both muscle phenotypes stem from the lack of LRT. In addition, similar phenotypes were also detected in 73% (*n*=15) of embryos in which LRT was knocked down by driving the expression of RNAi against *lrt* together with Dicer2, using the *actin-gal4* driver (Fig. 3D). The ubiquitous *actin-gal4* driver was used to enable expression of the RNAi construct at early embryonic stages to reduce the mRNA levels of *lrt* detected at stage 12. In cells not subjected to RNAi knockdown, expressing only the *actin-gal4* driver together with Dicer2, only 20% of the embryos showed abnormal VO4/VA3 extension in a single segment (*n*=16) (see also Table 1). Taken together, these experiments suggested that LRT is essential for the targeting of some of the ventral muscles towards their attachment sites and for the arrest of ectopic muscle extensions once the muscle reaches its corresponding tendon cell. Staining for PSβ-integrin showed that the myotendinous junction was established in the *lrt* mutant embryos in regions where muscles reached the tendon sites (arrows in Fig. 3E,F). However, in the ventral regions where muscles were missing, no integrin staining was detected (Fig. 3F, arrowhead), suggesting that lack of LRT does not directly affect the ability of the muscles to establish contacts with the tendon cells. Importantly, tendon cell markers, including Stripe and Shortstop were normally expressed in *Df(2R)BSC403*, indicating that tendon gene expression is not affected by non-related genes uncovered by the deficiency (Fig. 3G,H,IJ).

To further characterize the phenotype of the mutant embryos, we followed the morphology, migration and adhesion of a single muscle in *lrt* mutant embryos by recombining UAS-CD8GFP with the *5053-gal4* driver (expressed in muscle 12) on the background of *Df(2R)BSC403*. Whereas the majority of muscle 12 myotubes interacted normally with their corresponding tendon cells at the segmental border, we detected abnormally oriented membrane extensions of various sizes formed by this muscle (Fig. 4C,D arrows). These extensions were detected in 53% (*n*=23) of mutant embryos at stage 16 in at least one to two segments. Only embryos heterozygous for the 5053-gal4 driver were selected for this analysis as homozygous embryos carrying *5053-gal4* exhibit an aberrant muscle pattern. No heterozygous embryos exhibited the unique
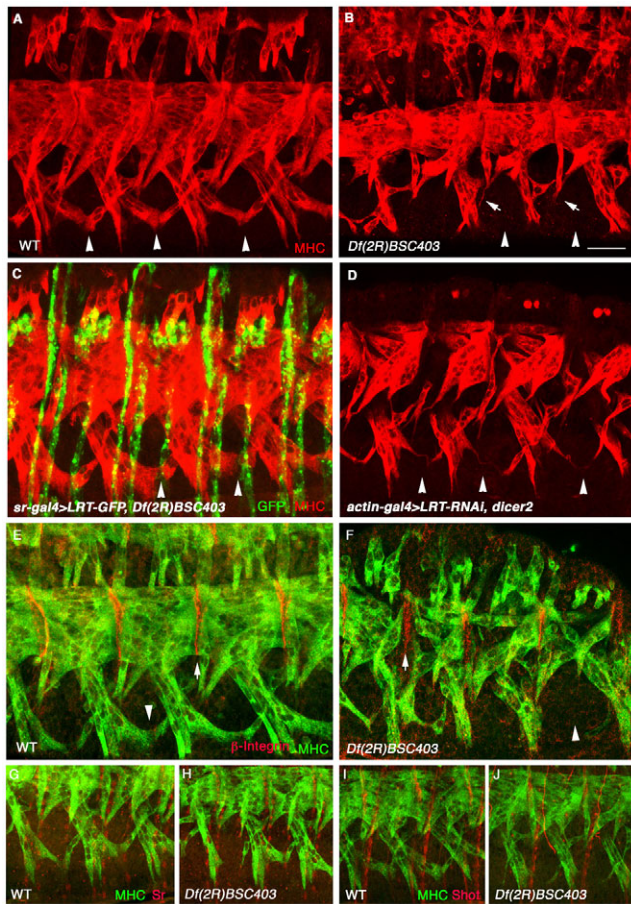
Fig. 3. LRT is essential for muscle targeting towards tendon cells.
(**A-F**) Wild-type (A,E) and *lrt* mutant [Df(2R)BSC403; B,C,F] embryos
labeled for MHC (red in A-D; green in E,F). Arrowheads in B indicate
the absence of VO4 and VA3 in the mutant embryo [compare with the
same muscles in wild type (arrowheads in A)]. Arrows in B indicate the
thin membrane extensions detected in the *lrt* mutant embryos.
(C) Rescue of the muscle phenotype by expression of LRT-GFP in tendon
cells of the mutant embryo. (D) RNAi specific to *lrt* driven by the *actin-
gal4* driver (arrowheads indicate the lack of proper VO4 and VA3
muscle extension, as compared with the rescued embryo in C).
(E,F) Wild-type (E) and *lrt* mutant (F) embryos, double-labeled for
Myosin heavy chain (MHC; green) and PSβ integrin (red). Arrows
indicate positive integrin labeling in E and F; arrowheads point to a lack
of integrin staining in the *lrt* mutant, and corresponding positive
staining in wild type (E). (**G,H**) Wild-type (G) or *lrt* mutant (H) embryos
stained for Stripe (red) and MHC (green). (**I,J**) Wild-type (I) or *lrt* mutant
(J) embryos stained for Shortstop (Shot, red) and MHC (green). Stripe
and Shot appear normal in *Df(2R)BSC403*. Scale bar: 20 μm in B.

phenotype of abnormal muscle extensions (*n*=11) (Fig. 4A,B).
Examination of embryos at an earlier developmental stage in which
muscle 12 had not arrived at its corresponding tendon cell revealed
that some of these muscles exhibited extra filopodia (Fig. 4F,
arrows). Significantly, the phenotype of abnormal muscle extensions
was rescued in 100% of the embryos (*n*=15) by the expression of
LRT-GFP in tendon cells, indicating that the phenotype resulted
from the lack of LRT (Fig. 4G,H) (see Table 1).

Thus, the lack of LRT leads to a failure of certain muscles to
locate their proper tendon cells, and in addition, causes muscles to
form misguided ectopic membrane extensions even before muscle
arrival at its target tendon cell.

Overexpression of LRT changes the directional migration of certain muscles

To further elucidate the function of LRT, we overexpressed the LRT-
GFP fusion protein in several different tissues. Although ectopic
expression of LRT in muscles (using the *mef2-gal4* driver) did not
change muscle migration behavior, its overexpression in tendon
cells led to a clear phenotype in which in 70% of the embryos (*n*=12)
the dorsal longitudinal muscles stalled close to a single segmental
border and did not extend between two segmental borders in two to
four segments (Fig. 5D, arrow). In 20% of these embryos, we also
detected similar defects in the ventral longitudinal muscles (Fig. 5C,
arrow). In wild-type embryos, both dorsal and ventral longitudinal
muscles form their initial contact with tendon cells at one side of the
segment and then extend in the opposite direction, often to a tendon
cell located at the more anterior segmental border. It appeared that
overexpression of LRT led to stalling of the muscle in the proximity
of the initial segmental border, with the muscle presumably unable
to extend to the more anterior attachment site. Embryos
heterozygous for *sr-gal4* did not show the ventral stalling muscle
phenotype (*n*=10), and only 8% showed a dorsal stalling muscle
phenotype (*n*=11) (see Table 1).

The stalled muscles often did not establish integrin-mediated
adhesion with tendon cells, and the characteristic continuous line of
integrin staining along the segmental border was missing or
interrupted in LRT-overexpressing embryos (Fig. 5G, arrowhead).
This suggests that the stalled muscles do not establish normal
adhesion with their corresponding tendon cells.

In conclusion, elevating the levels of LRT in tendon cells
prevented proper extension of certain muscles towards their
attachment sites, inhibiting their ability to stretch between two
segmental borders.

LRT forms a protein complex with Robo receptors

The non-autonomous effect of LRT on muscle migration behavior
suggested that muscles might express a putative receptor for LRT.
The leucine-rich repeat domain of LRT is similar to the second LRR
domain of Slit. This domain in Slit was demonstrated to interact with
Robo receptors (Hohenester, 2008; Howitt et al., 2004; Morlot et al.,
2007). Importantly, the muscle phenotype of Slit and Robo mutant
embryos resembles that of LRT overexpression (Kramer et al., 2001)
(Fig. 7C). We therefore hypothesized that LRT might interact with
Robo through its LRR domain. To test this possibility, S2 cells were
first transfected with LRT-GFP alone. The GFP labeling appeared to
be associated with the plasma membrane (Fig. 6A). We noticed that
part of the LRT-GFP was retained inside the S2 cell, presumably
representing vesicle and/or ER staining. Co-transfection with both
Robo-HA and full-length LRT-GFP indicated that LRT-GFP co-
localized with Robo-HA at the surfaces of the plasma membrane of
the S2 cells (Fig. 6B,C,D). To verify that LRT-GFP was indeed
localized at the plasma membrane, we treated live S2 cells
transfected with LRT-GFP with Trypsin; the protease activity was
then stopped by the addition of serum, and we analyzed the cell
extract by western analysis for GFP. The levels of the intact LRT-
GFP band (molecular weight =130 kDa) were significantly reduced
and a new 30 kDa band appeared, corresponding in size to the
truncated cytoplasmic LRT-GFP domain (Fig. 6J). This experiment
verifies that LRT is indeed a transmembrane protein.

Next, a soluble form of LRT-GFP, including the full extracellular
domain of LRT fused to GFP, was produced (LRT-NTD) and
transfected into S2 cells. The conditioned medium of these cells,
containing the secreted LRT-GFP protein, was collected and cleared
from floating cells by centrifugation. It was then added to S2 cells

Table 1. Quantitative analysis of the phenotypes of *lrt* mutants and LRT overexpressing embryos

A. Quantitative summary of the *lrt* mutant phenotype

	VO4/VA3				Muscle 12		
	WT	RNAi	Df(2R) BSC403	Rescue	WT	Df(2R) BSC403	Rescue
Number of embryos affected in 2-4 segments	0 (n=42)	15 (n=21; P=0.000001)	11 (n=15; P=7×10^{-9})	0 (n=11; P=0.015)	0 (n=11)	13 (n=23; P=0.02)	0 (n=15; P=0.005)

B. Quantitative summary of the LRT overexpression phenotype

	Number of affected WT embryos	Number of affected LRT overexpressing embryos
Dorsal 2-4 segments	1 (n=12)	9 (n=12; P=0.05)
Ventral longitudinal 2-3 segments	0 (n=10)	4 (n=17; P=0.2)

transfected with Robo-HA. Strikingly, LRT-GFP accumulated specifically on the surfaces of the Robo-HA expressing cells, but not on non-transfected S2 cells (Fig. 6E-H). This experiment suggested that LRT associates specifically with Robo on the plasma membrane of S2 cells. Moreover, co-immunoprecipitation of LRT-GFP and Robo-HA was performed on an extract of S2 cells co-transfected with both Robo-HA and LRT-GFP using immobilized anti-GFP

antibodies. Western analysis of an extract of these beads showed that Robo-HA co-precipitated specifically with LRT-GFP but not on immobilized anti-GFP antibodies in the absence of LRT-GFP, indicating that these proteins indeed form a protein complex in S2 cells (Fig. 6I).

Genetic interaction between LRT and Robo

To address whether LRT and Robo interact at a functional level during the formation of muscle-tendon attachment, we tested whether reducing Robo levels (e.g. in embryos heterozygous for Robo expression) could reverse the gain of function phenotype observed following overexpression of LRT in tendon cells (shown in Fig. 5). Significantly, a complete rescue was detected in 100% of embryos heterozygous for Robo and overexpressing LRT-GFP in tendons (n=13) (Fig. 7 compare B to A), indicating that LRT acts through Robo receptor(s) and pointing to a functional relationship between LRT and Robo. Furthermore, reducing the levels of Robo, Robo2 and Robo3 in muscles by driving muscle-specific expression of an RNAi directed to all three genes, using the *mef2-gal4* driver, led to an abnormal muscle pattern in which the muscles failed to extend at either end to the segmental border tendon cells. This phenotype resembled that of the LRT overexpression phenotype described above (see Fig. 5) and was detected in 47% (n=15) of the mutant embryos (Fig. 7C). Importantly, when co-expressing LRT-GFP together with the Robo RNAi constructs in the muscles, the muscle phenotype was detected in only 11% of the embryos (n=9) (Fig. 7D), suggesting that LRT potentiates Robo activity when expressed in muscles. Of note is that overexpressing LRT-GFP alone in muscles did not result in any muscle phenotype (see Fig. 2). When examining embryos trans-heterozygous for *Df(2R)BSC403* and *robo* we did not observe defects in the muscle pattern.

Taken together, these experiments suggest functional relationships between LRT and Robo receptors.

DISCUSSION

When migrating cells encounter their target tissue they must arrest their migration behavior. Signals promoting arrest of cell migration are yet to be elucidated. Here we describe the identification of a novel leucine-rich repeat protein, LRT, expressed specifically by tendon cells downstream of Stripe activity, and capable of associating with muscle-expressed Robo receptors. We further demonstrated that LRT acts non-autonomously on muscles to promote proper muscle-tendon assembly by arresting muscle filopodia formation following the arrival of the muscle at the tendon cell. This activity is presumably achieved by an interaction between LRT on the tendon cell and Robo receptors on the migrating muscle cell.
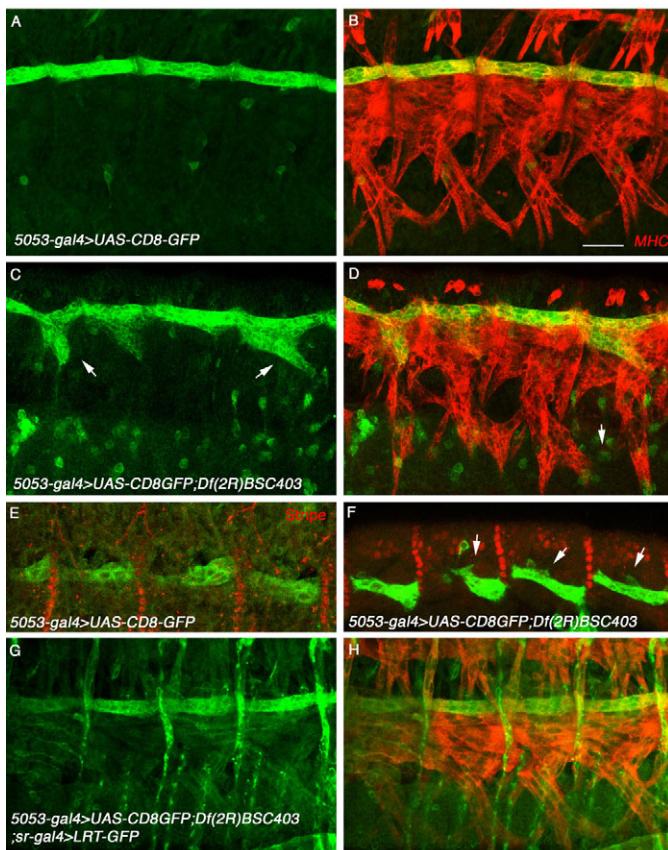

Fig. 4. Lack of LRT leads to ectopic muscle extensions.
(**A-H**) Embryos at stage 16 (A-D,G,H) or at stage 13-14 (E,F) carrying the *5053-gal4* and *UAS-CD8-GFP* on a wild-type background (A,B,E), in homozygous *Df(2R)BSC403* (C,D,F), or in homozygous *Df(2R)BSC403* together with *sr-gal4 and UAS-LRT-GFP* (G,H). GFP appears in green (A-F); Myosin heavy chain is in red (B,D,F). Arrows in C indicate uncoordinated muscle extensions. Arrow in D shows the abnormal extension of muscle VO4 and VA3. The arrows in F indicate muscle extensions. (G,H) Rescue of abnormal extensions by LRT-GFP expression. Scale bar: 20 μm in B.
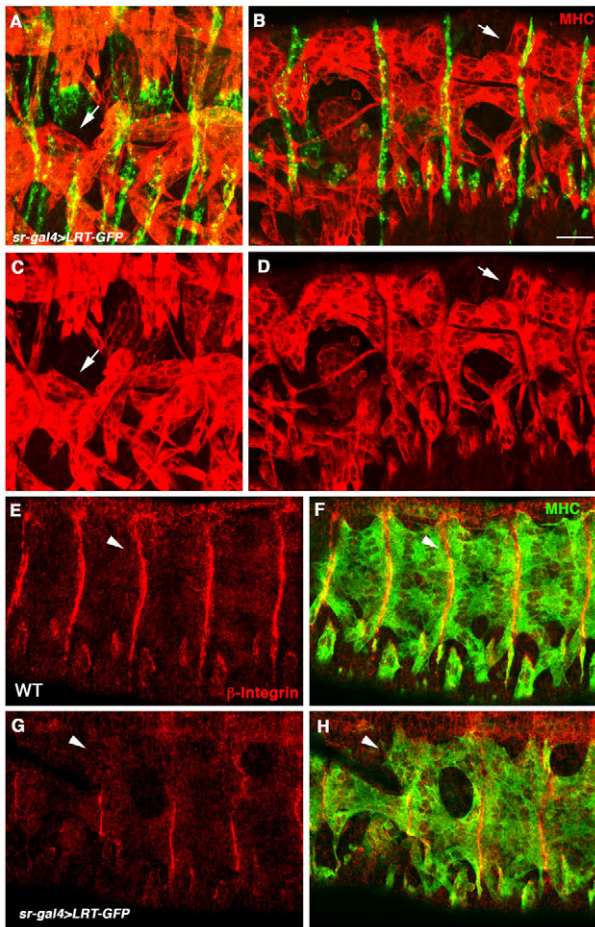
Fig. 5. Overexpression of LRT in tendon cells leads to a stalled muscle phenotype. (**A-D**) Embryo overexpressing LRT-GFP driven by *sr-gal4* stained for GFP (green, A,B) and for Myosin heavy chain (MHC; red). The arrows indicate stalled muscles. (**E-H**) Wild-type embryo (E,F) or embryo overexpressing LRT-GFP driven by *sr-gal4* (G,H) labeled for β-integrin (red) and MHC (green, F,H). Arrowheads in E,F indicate the continuous line of β-integrin staining at the segmental border and in G,H indicate the lack of β-integrin staining in regions of stalled muscles. Scale bar: 20 μm in B.

Fig. 6. LRT forms a protein complex with Robo. (**A-H**) S2 cells transfected with LRT-GFP alone (green, A) or LRT-GFP (green, B) together with Robo-HA (red, anti-HA, C). D is the merged image of B and C. Arrow in A indicates the surface of the S2 cell; arrows in B-D represent surface co-labeling of LRT-GFP and Robo-HA. (E) S2 cell reacted with conditioned medium containing the extracellular domain of LRT fused to GFP (NTD-GFP); (F-H) S2 cells transfected with Robo-HA (red, anti-HA in G,H) and reacted with conditioned medium of the extracellular domain of LRT fused to GFP (NTD-GFP). H is the merged image of F and G. Arrowheads indicate the specific accumulation of NTD-GFP on the surface of a cell expressing Robo-HA. (**I**) Co-immunoprecipitation of LRT-GFP from S2 cells co-transfected with Robo-HA and LRT-GFP. Crude extract of these cells reacted with anti-HA or with anti-GFP is shown in the first (left-hand) lane. The second lane represents immunoprecipitation of S2 cells transfected with Robo-HA alone, precipitated with immobilized anti-GFP antibodies, and reacted with anti-HA as well as with anti-GFP antibodies. The third lane represents cells co-transfected with Robo-HA and LRT-GFP, whose extract (shown in the first lane) was precipitated with immobilized anti-GFP antibodies and reacted with both anti-HA and anti-GFP antibodies. Robo-HA and LRT-GFP are detected. (**J**) Trypsin non-treated (left lane) and treated (right lane) extract of S2 cells transfected with LRT-GFP. Arrowheads point to the intact LRT-GFP band of 130 kDa (reduced after Trypsin treatment), the truncated cytoplasmic domain of LRT fused to GFP (CTD-GFP) band of 30 kDa (appeared following Trypsin treatment), and a non-specific band of 25 kDa (equally detected in both lanes).

LRT protein was detected at relatively late stages of embryonic development following muscle attachment to tendon cells. This suggests that it does not function primarily to guide muscles to their attachment sites, but rather is required for the arrest of muscle extension and/or migration behavior. Two possible mechanisms may account for the arrest of muscle migration behavior: a specific signal provided by the tendon cell promoting the end of filopodia formation, or alternatively the establishment of the myotendinuous junction, which alters the leading edge morphology of the muscle cell so that it is no longer forming filopodia. Lack of LRT led to ectopic membrane extensions in various ventral oblique and acute muscles as well as in muscle 12, whereas in some muscles (e.g. VO4 or VA3), the continuous formation of muscle extensions in mutant embryos led to a failure to form proper muscle-tendon contacts. In other muscles (e.g. muscle 12) these extra-muscle extensions did not affect contact formation with the tendon cells. This latter phenotype supports a model by which a contact-independent signal promotes the arrest of muscle migration behavior. The expression of LRT on the surface of the tendon cell might represent such a signal.
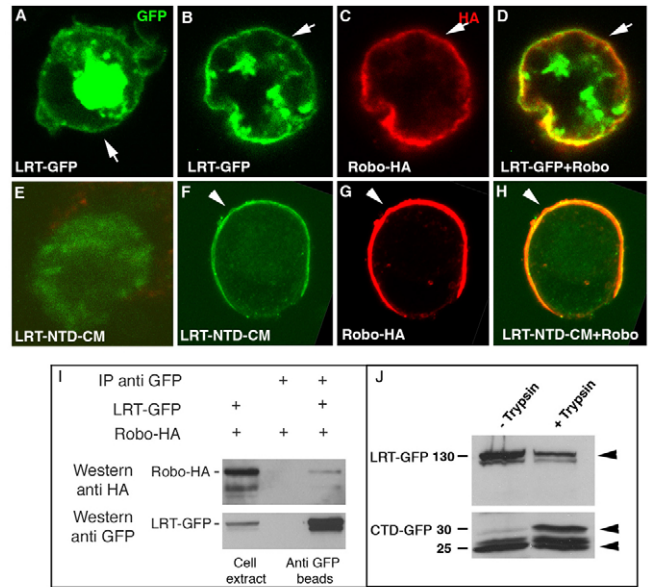
LRT may mediate the arrest of these extraneous membrane extensions by interacting with a receptor on the muscle, which, upon binding, represses the formation of further membrane extensions. Alternatively, LRT may compete for binding to a common receptor with an attractive signal provided by the tendon cell. Association of LRT with such a receptor may dampen further signaling required for the continuous extension of the muscle leading edge. In both scenarios, overexpression of LRT in tendon cells is likely to result in a stronger association of the muscle with the proximal tendon cell, inhibiting muscle extension to the more distal tendon by arresting its filopodia formation. This phenotype was indeed observed when LRT was overexpressed in tendon cells. The muscles with extension that was arrested failed to form a proper myotendinous junction.
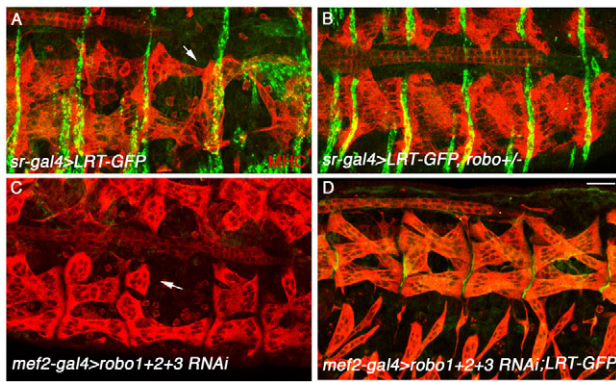
Fig. 7. Functional relationships between LRT and Robo in muscle cells. (**A-D**) Embryo overexpressing LRT-GFP driven by the *sr-gal4* driver in a stage 16 wild-type embryo (A), or in an embryo at the same stage, heterozygous for *robo* (B). LRT-GFP (green, A,B,D) and Myosin heavy chain (MHC; red) are shown. (C) Dorsal view of an embryo expressing RNAi constructs for Robo 1, 2 and 3 driven by *mef2-gal4*. (D) A similar embryo expressing both the RNAi constructs for Robo 1, 2 and 3 as well as LRT-GFP. The arrows in A and C indicate the stalled muscles. Scale bar: 20 μm in D.

A possible mechanism by which LRT might act is through its interaction with the Robo receptors. Robo mediates attractive activity between the muscles and tendon cells (Kramer et al., 2001). We demonstrated here that LRT associates with the extracellular domain of Robo. In addition, we detected a reciprocal interaction between LRT and Robo, in which reducing Robo levels could rescue the muscle-stalling phenotype of LRT overexpression. This experiment suggests that LRT promotes muscle stalling through an interaction with Robo receptors. In addition, overexpression of LRT in muscles partially rescued the Robo knockdown phenotype, which is consistent with LRT potentiating Robo activity when co-expressed in the muscle. We further tested whether LRT affects the distribution of Robo receptors along the muscle membrane; however, we did not detect a major difference between Robo distribution or expression levels in *Df(2R)BSC403*, LRT-overexpressing, or wild-type embryos (not shown). Alternatively, LRT may inhibit ectopic membrane extensions by reducing the levels of free Robo receptors by either direct interaction with these receptors, or by association with additional muscle surface proteins required for Robo-Slit signaling.

If LRT inhibits Robo-Slit interactions, its expression at the ventral midline should inhibit muscle repulsion from this domain. Ectopic expression of LRT-GFP using the midline driver *slit-gal4* slightly affected the pattern of the ventral muscles, and these muscles appeared to extend closer to the midline (see Fig. S2 in the supplementary material), suggesting that LRT counteracts Robo-mediated repulsion of the muscles in the midline. We did not observe a notable effect on the pattern of the central nervous system axons following LRT ectopic expression in the midline (Fig. S2 in the supplementary material). This could be due to additional mechanisms regulating Robo distribution on the axonal membrane.

LRR proteins expressed on distinct tissues share a common function in cell-cell recognition events as well as in the regulation of membrane extensions (Milan et al., 2002; Sakurai et al., 2007). In recent years, several *Drosophila* LRR proteins were demonstrated to affect targeting of motor axons and of specific muscles (Kohsaka and Nose, 2009; Kurusu et al., 2008). Intriguingly, simultaneous labeling of the presynaptic and postsynaptic sites showed that,

before synapse formation, muscle membrane extensions called myopodia express the LRR protein Capricious at their tips (Kohsaka and Nose, 2009). These myopodia tips interact with axonal tips in order to form a properly located synapse. The axonal receptor for Capricious has not yet been identified. Based on our studies, Robo receptors at the axon tips may interact directly with Capricious at the muscle myopodia. Similarly to LRT-mediated arrest of filopodia formation at the muscle tips, LRR proteins on the muscle myopodia may promote the arrest of the axonal tip formation to enable synapse formation.

In summary, we have identified a novel tendon-specific surface protein, which is essential for arresting ectopic muscle filopodia formation following the arrival of the muscle at its targeted tendon cell, thereby promoting targeting of muscles to tendon cells. LRT may act by modulating Robo-Slit interactions, which are essential for the correct guidance of muscles to their specific tendon-mediated insertion sites.

Supplementary material
Supplementary material for this article is available at
http://dev.biologists.org/cgi/content/full/136/21/3607/DC1
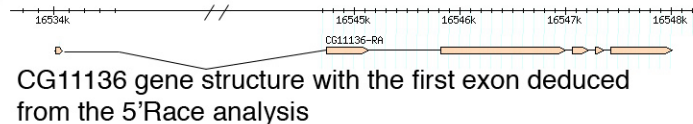
References
Becker, S., Pasca, G., Strumpf, D., Min, L. and Volk, T. (1997). Reciprocal signaling between Drosophila epidermal muscle attachment cells and their corresponding muscles. *Development* **124**, 2615-2622.
Bella, J., Hindle, K. L., McEwan, P. A. and Lovell, S. C. (2008). The leucine-rich repeat structure. *Cell Mol. Life Sci.* **65**, 2307-2333.
Blair, S. S. (2001). Cell lineage: compartments and Capricious. *Curr. Biol.* **11**, R1017-R1021.
Bokel, C. and Brown, N. H. (2002). Integrins in development: moving on, responding to, and sticking to the extracellular matrix. *Dev. Cell* **3**, 311-321.
Chanana, B., Graf, R., Koledachkina, T., Pflanz, R. and Vorbruggen, G. (2007). AlphaPS2 integrin-mediated muscle attachment in Drosophila requires the ECM protein Thrombospondin. *Mech. Dev.* **124**, 463-475.
Dickson, B. J. and Gilestro, G. F. (2006). Regulation of commissural axon pathfinding by slit and its Robo receptors. *Annu. Rev. Cell Dev. Biol.* **22**, 651-675.
Dolan, J., Walshe, K., Alsbury, S., Hokamp, K., O'Keeffe, S., Okafuji, T., Miller, S. F., Tear, G. and Mitchell, K. J. (2007). The extracellular leucine-rich repeat superfamily; a comparative survey and analysis of evolutionary relationships and expression patterns. *BMC Genomics* **8**, 320.
Frommer, G., Vorbruggen, G., Pasca, G., Jackle, H. and Volk, T. (1996). Epidermal egr-like zinc finger protein of Drosophila participates in myotube guidance. *EMBO J.* **15**, 1642-1649.
Hohenester, E. (2008). Structural insight into Slit-Robo signalling. *Biochem. Soc. Trans.* **36**, 251-256.
Howitt, J. A., Clout, N. J. and Hohenester, E. (2004). Binding site for Robo receptors revealed by dissection of the leucine-rich repeat region of Slit. *EMBO J.* **23**, 4406-4412.
Kohsaka, H. and Nose, A. (2009). Target recognition at the tips of postsynaptic filopodia: accumulation and function of Capricious. *Development* **136**, 1127-1135.
Kramer, S. G., Kidd, T., Simpson, J. H. and Goodman, C. S. (2001). Switching repulsion to attraction: changing responses to slit during transition in mesoderm migration. *Science* **292**, 737-740.
Krause, C., Wolf, C., Hemphala, J., Samakovlis, C. and Schuh, R. (2006). Distinct functions of the leucine-rich repeat transmembrane proteins capricious and tartan in the Drosophila tracheal morphogenesis. *Dev. Biol.* **296**, 253-264.
Kurusu, M., Cording, A., Taniguchi, M., Menon, K., Suzuki, E. and Zinn, K. (2008). A screen of cell-surface molecules identifies leucine-rich repeat proteins as key mediators of synaptic target selection. *Neuron* **59**, 972-985.
Milan, M., Weihe, U., Perez, L. and Cohen, S. M. (2001). The LRR proteins capricious and Tartan mediate cell interactions during DV boundary formation in the Drosophila wing. *Cell* **106**, 785-794.
Milan, M., Perez, L. and Cohen, S. M. (2002). Short-range cell interactions and cell survival in the Drosophila wing. *Dev. Cell* **2**, 797-805.

Milan, M., Perez, L. and Cohen, S. M. (2005). Boundary formation in the Drosophila wing: functional dissection of Capricious and Tartan. *Dev. Dyn.* **233**, 804-810.

Morlot, C., Thielens, N. M., Ravelli, R. B., Hemrika, W., Romijn, R. A., Gros, P., Cusack, S. and McCarthy, A. A. (2007). Structural insights into the Slit-Robo complex. *Proc. Natl. Acad. Sci. USA* **104**, 14923-14928.

Sakurai, K. T., Kojima, T., Aigaki, T. and Hayashi, S. (2007). Differential control of cell affinity required for progression and refinement of cell boundary during Drosophila leg segmentation. *Dev. Biol.* **309**, 126-136.

Schnorrer, F. and Dickson, B. J. (2004). Muscle building: mechanisms of myotube guidance and attachment site selection. *Dev. Cell* **7**, 9-20.

Steigemann, P., Molitor, A., Fellert, S., Jackle, H. and Vorbruggen, G. (2004). Heparan sulfate proteoglycan syndecan promotes axonal and myotube guidance by slit/robo signaling. *Curr. Biol.* **14**, 225-230.

Subramanian, A., Wayburn, B., Bunch, T. and Volk, T. (2007). Thrombospondin-mediated adhesion is essential for the formation of the myotendinous junction in Drosophila. *Development* **134**, 1269-1278.

Volk, T. (1992). A new member of the spectrin superfamily may participate in the formation of embryonic muscle attachments in Drosophila. *Development* **116**, 721-730.

Volk, T. (1999). Singling out Drosophila tendon cells: a dialogue between two distinct cell types. *Trends Genet.* **15**, 448-453.

Volk, T. and VijayRaghavan, K. (1994). A central role for epidermal segment border cells in the induction of muscle patterning in the Drosophila embryo. *Development* **120**, 59-70.

Volohonsky, G., Edenfeld, G., Klambt, C. and Volk, T. (2007). Muscle-dependent maturation of tendon cells is induced by post-transcriptional regulation of stripeA. *Development* **134**, 347-356.

Vorbruggen, G. and Jackle, H. (1997). Epidermal muscle attachment site-specific target gene expression and interference with myotube guidance in response to ectopic stripe expression in the developing Drosophila epidermis. *Proc. Natl. Acad. Sci. USA* **94**, 8606-8611.

Williams, G. J. and Caveney, S. (1980). Changing muscle patterns in a segmental epidermal field. *J. Embryol. Exp. Morphol.* **58**, 13-33.
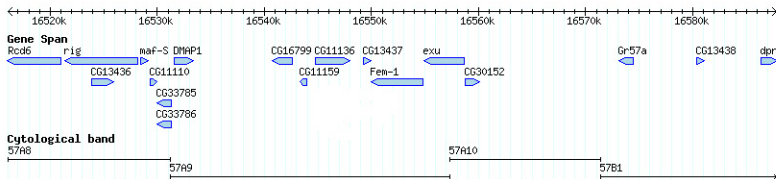
DEVELOPMENT

A

CG11136 gene structure (FlyBase)

B

CG11136-RA

CG11136 gene structure with the first exon deduced
from the 5'Race analysis

C

Df(2R)BSC404

A *slit-gal4*

B *slit-gal4::UAS-LRT*

C MHC Wrapper

D